Nanotechnology **19** (2008) 335707 (6pp) doi:10.1088/0957-4484/19/33/335707

Functionalizing graphene by embedded boron clusters

Alexander Quandt[1,5], **Cem Özdoğan**[2], **Jens Kunstmann**[3] and **Holger Fehske**[4]

[1] CNR–IFN Trento, CSMFO group, Via Alla Cascata 56/c, 38050 Povo-Trento, Italy
[2] Department of Computer Engineering, Çankaya University, Balgat, 06530 Ankara, Turkey
[3] Max-Planck-Institut für Festkörperforschung, Heisenbergstrasse 1, 70569 Stuttgart, Germany
[4] Institut für Physik der Universität Greifswald, Felix-Hausdorff-Straße 6, 17489 Greifswald, Germany

E-mail: quandt@physik.uni-greifswald.de

Received 29 April 2008, in final form 30 April 2008
Published 8 July 2008
Online at stacks.iop.org/Nano/19/335707

Abstract

We present a model system that might serve as a blueprint for the controlled layout of graphene based nanodevices. The systems consists of chains of B_7 clusters implanted in a graphene matrix, where the boron clusters are not directly connected. We show that the graphene matrix easily accepts these alternating B_7-C_6 chains and that the implanted boron components may dramatically modify the electronic properties of graphene based nanomaterials. This suggests a functionalization of graphene nanomaterials, where the semiconducting properties might be supplemented by parts of the graphene matrix itself, but the basic wiring will be provided by alternating chains of implanted boron clusters that connect these areas.

(Some figures in this article are in colour only in the electronic version)

Single layers of graphite called graphene are the precursors of carbon nanotubes [1], which are one of the key materials for nanotechnology. However, since the discovery of stable multi-layers and single layers of graphene [2], the latter quickly shifted into the focus of nanotechnology as well. For carbon nanotubes a simple tight-binding scheme [3] predicts that they should either be semiconducting or metallic, depending on their chirality [1]. The same theory predicts that stripes cut from bulk graphene may either be semiconducting or metallic, depending on the nature of their boundaries [4][6].

However, a broad semiconducting sheet of graphene could be a suitable basis on which to build an ultimate two-dimensional nanoelectronic technology. This would require a controlled wiring of such devices on the nanoscale, which has little to do with the clumsy state-of-the-art wiring of graphene devices made for the purpose of basic scientific investigations. In fact the tiny wiring necessary for technologically relevant nanoelectronic applications of graphene must primarily be based on a chemistry that is largely compatible with carbon chemistry, and the purpose of this paper is to suggest such a system.

In the field of nanotubes, it has been shown that boron nanotubes are largely compatible with carbon nanotubes [5]. In particular, interfaces between boron and carbon nanotubes were shown to be stable [6]. The basis for this compatibility must be sought in the electron deficient nature of boron, which leads to a complex, but somewhat adjustable multi-centered bonding. Another favorable property of electron deficient elements like boron is their ability to force other elements into unusually high coordinations [7]. This property should allow for a certain range of structural adjustments to be made whenever boron fragments are in touch with a carbon environment, as seen in the case of nanotubular interfaces [6] or mixed boron–carbon clusters [8].

Finally it turns out that small boron clusters are quasi-planar, and largely made from pyramidal B_7-units [9]. The same building blocks are the basis of novel boron nanomaterials, including boron nanotubes or boron sheets [5, 10], the latter being the boron equivalent of graphene. Interestingly enough, all bulk boron nanomaterials made from these B_7-units are metallic. Now from a pure geometrical point of view, a quasi-planar boron cluster made from B_7-units would fit quite

[5] Permanent address: Institut für Physik der Universität Greifswald, Felix-Hausdorff-Straße 6, 17489 Greifswald, Germany.
[6] These standard results were verified using a MAPLE 9.5 worksheet developed by one of us (AQ).

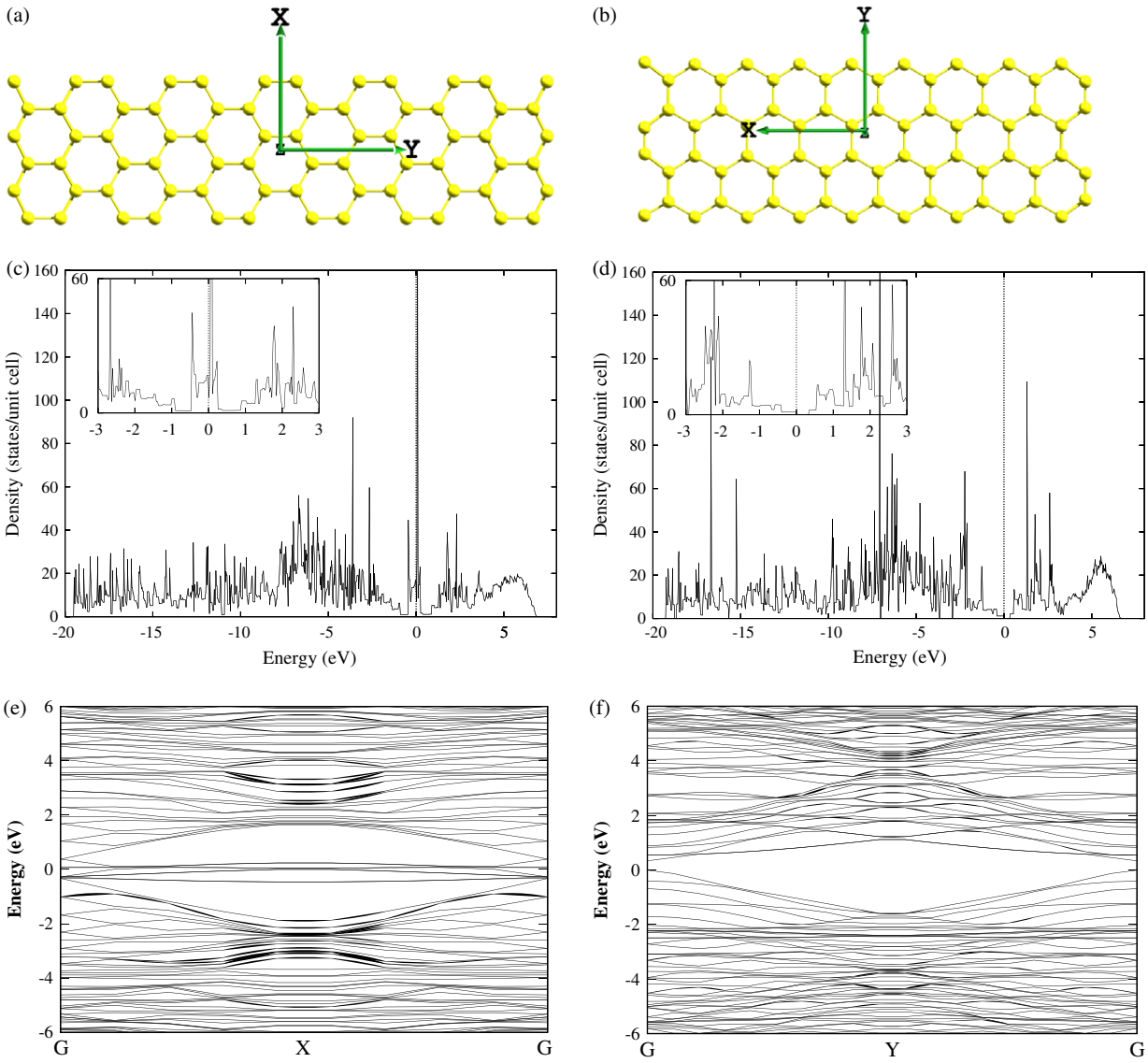

Figure 1. Graphene nanoribbons. Figure shows relaxed structure of (a) zigzag nanoribbon and (b) armchair nanoribbon, where the horizontal direction spans the width of the ribbon, and the vertical direction corresponds to the periodic direction of the systems. The density of states for (c) a zigzag nanoribbon, which shows metallic behavior, and for (d) an armchair nanoribbon, which shows semiconducting behavior, as predicted by tight-binding theory [3, 4]. The insets show details of the density of states around the Fermi level located at 0 eV, and the Fermi level has been emphasized by a vertical bar. Electronic bands are drawn in the k_x-direction for (e) a zigzag nanoribbon, and in the k_y-direction for (f) an armchair nanoribbon. *G* denotes the gamma-point of the Brillouin zone.

perfectly into the honeycomb lattice, as a carbon honeycomb may also be seen as the basis of a hexagonal pyramidal C_7-unit, where the carbon at the top of the carbon pyramid has been removed.

But pure geometric arguments are not sufficient to establish boron as a suitable wiring component for graphene based nanotechnologies. We must also require chemical compatibility between the carbon matrix and implanted boron fragments. To this end, we have developed a suitable model system, and studied its basic structural and electronic properties using *ab initio* methods.

These *ab initio* calculations and optimizations were carried out using the VASP package (version 4.6.28) [11, 12], which is a density functional theory (DFT) based [13] *ab initio* code using plane wave basis sets and a supercell approach to model solid materials, surfaces, or clusters [14]. In our case, where all the systems should effectively be two-dimensional (i.e. monolayers), we were choosing supercells that allowed for a huge distance at right angles to these layers (i.e. the *z*-direction in figures 1 and 2). For the nanoribbons considered later on, we would also choose another huge distance in the direction of the width of those nanoribbons.

During our simulations, the electronic correlations were treated within the local-density approximation (LDA) using the Perdew–Zunger [15] form of the Ceperley–Alder exchange–correlation functional [16], and the ionic cores of the system were represented by ultrasoft pseudopotentials [17] as supplied by Kresse and Hafner [18]. The *k*-space integrations were

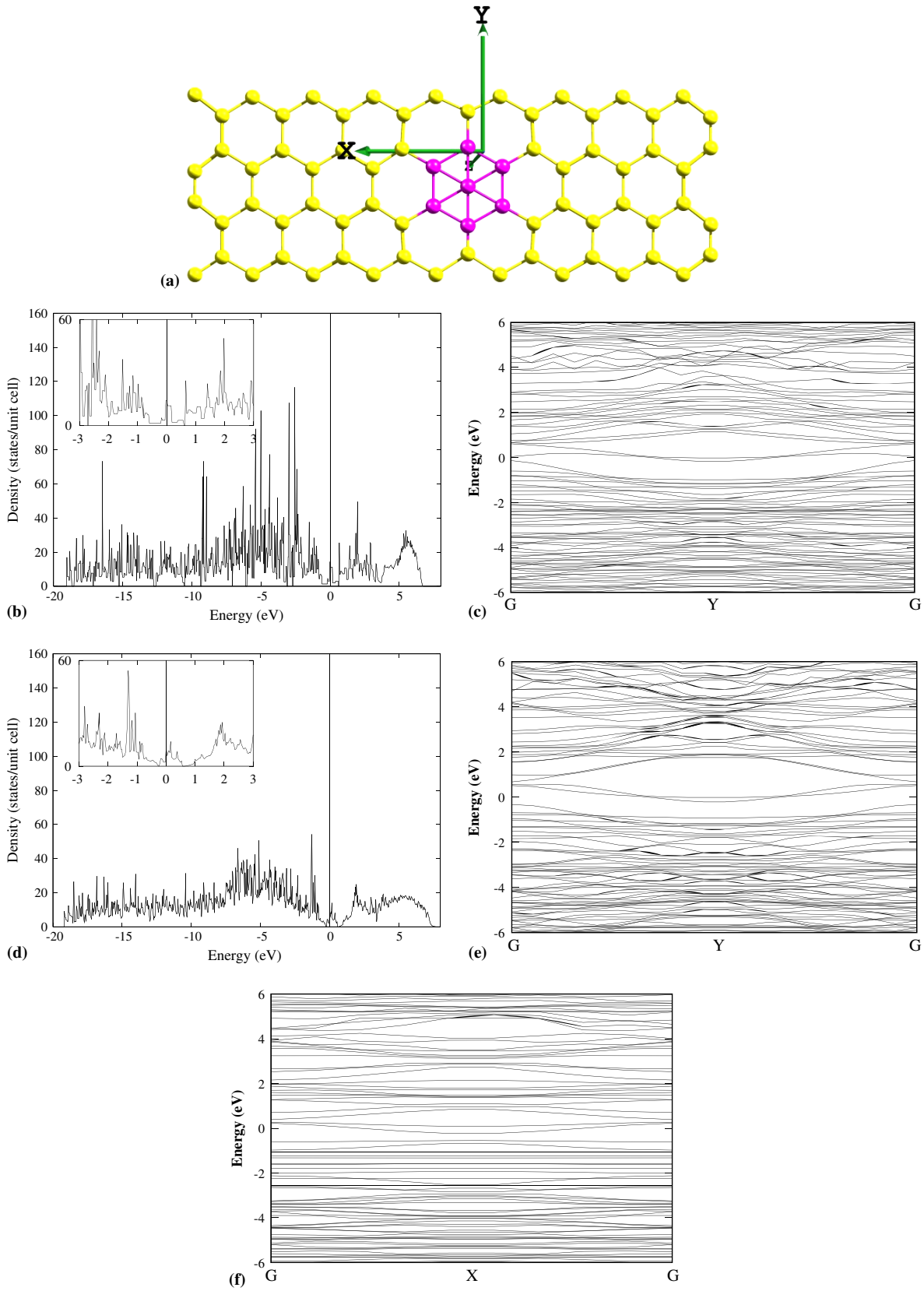

Figure 2. Boron doped graphene nanostructures. (a) Relaxed structure of boron doped armchair graphene, where the vertical y-direction corresponds to the periodic direction of the system. This structure is characterized by an alternating chain of B_7 clusters (shown in dark) along the y-direction, separated by a carbon honeycomb. The relaxed structure of boron doped graphene looks rather similar, but it is periodic in both the horizontal (x) and the vertical (y) direction. (b) Density of states for doped armchair graphene, which shows metallic behavior. (c) Electronic bands in the k_y-direction that show the corresponding band overlap at the Fermi level. (d) Density of states for boron doped graphene, similar to (b). (e)–(f) Electronic bands in the k_y- and k_x-direction for boron doped graphene.

Table 1. Number of atoms per unit cell and cohesive energies for various doped and non-doped graphene based nanomaterials. Note that for the zigzag and armchair nanoribbons, the system with a minimal unit cell labeled by 1 and the system with a doubled or tripled unit cell labeled by 2 describe the same physical system, which explains why the cohesive energies are practically identical.

Name	Number of atoms per unit cell	Cohesive energy in eV/atom
Graphene	2	−10.133
Zigzag ribbon 1	24	−9.830
Zigzag ribbon 2	72	−9.832
Armchair ribbon 1	36	−9.868
Armchair ribbon 2	72	−9.864
Doped armchair ribbon	73	−9.505
Doped graphene	73	−9.758

carried out using the method of Methfessel and Paxton [19] in first order, where we employed a smearing width of 0.1 eV. The optimal sizes of the k-point meshes for different systems were individually converged, such that changes in the cohesive energy were reduced to less than 3 meV/atom.

The structures were fully relaxed including lattice parameters and ions. In order to wash out the energy landscape in the search for global minima, and in order to prevent our quasi-two-dimensional systems from collapsing into multi-layered configurations during structure optimization, we ran VASP for a number of ionic steps with reduced precision (using only half of the converged k-point meshes), followed by a reset of the huge lattice parameters of the unit cell. This procedure was repeated several times.

Following these pre-relaxations, we restricted the structure optimizations to comprise the ionic degrees of freedom, only, but this time we used the optimal size of the k-point meshes[7]. The optimized systems finally underwent a series of static calculations, where we applied the tetrahedron method [20] for k-point sampling. At this stage, we checked that the stress on the system and the interatomic forces were sufficiently small, in order to obtain the accurate cohesive energies listed in table 1, and accurate band structures shown in figures 1 and 2. The density of states of the systems shown in figures 1 and 2 were obtained in a static run using four times the optimal size of the k-point meshes, in order to guarantee the proper resolution of small details.

In figure 1, we see the results of such simulations for graphene nanoribbons with zigzag and armchair borders. In the vertical direction of figures 1(a) and (b), the systems repeat themselves periodically, whereas in the horizontal direction, the ribbons just span the width shown in these pictures, and a neighboring nanoribbon to the right or to the left of it will be too far away to interact with this strip. Note that the smallest unit cells for these systems comprised only one third of the atoms shown in the zigzag case, and one half of the atoms shown in the armchair case. However, we extend the unit cells in order to be sure that our general procedures would remain valid in the size ranges that we would finally choose for the doped model to be discussed below. The near identical cohesive energies for all settings, and the comparison of these energies with the cohesive energy of graphene listed in table 1, were a strong indication that our basic procedure for carrying out *ab initio* simulations on such systems was reliable.

Tight-binding theory [3, 4] predicts all zigzag nanoribbons to be metallic, and this result is confirmed by the results shown in figures 1(c) and (e). In the case of an armchair nanoribbon the same theory predicts all of these structures to be semiconducting, unless the number of dimers from one border of the nanoribbon to the other is $3n - 1$, with n being a natural number. We see, however, that the number of dimers in figure 1(b) is 18, and therefore this nanoribbon should be semiconducting, which is confirmed by the results displayed in figures 1(d) and (f).

With the semiconducting armchair system shown in figure 1, we found an ideal starting point for setting up a model system that contains (alternating) chains of boron clusters running in the periodic direction of a semiconducting nanoribbon. But the question was, which kind of system should be examined in the first place? One might certainly think of starting with single boron atoms laid out in the periodic direction. Such studies have already been carried out quite recently [21], and the authors observed that single boron atoms have a strong tendency to diffuse to the borders of the nanoribbons, similar to boron migration in open-ended boron doped carbon nanotubes [22]. Thus, although this type of doping might be very important for spin transport through graphene nanoribbons, which seems to be mediated by edge states, it was of little help for our goal to find a model that would describe the bulk functionalization of a broad semiconducting graphene nanoribbon.

Therefore we decided to insert something as large as boron clusters made from pyramidal B_7-units, which might not diffuse that easily to the open ends of a graphene nanoribbon. Note that for microelectronic devices close to the lithographic limit and beyond, there is a similar trend towards the implantation of boron clusters instead of boron atoms [23], because with shrinking system sizes, single boron atoms become too mobile, and the MOSFET devices will degrade too quickly. There is no reason to assume that this situation would be any better in the case of graphene based devices.

To avoid these problems, the necessary implantation machines for boron clusters are already available (see [23]). Therefore a first step towards the realization of our model system could be to shine an intense beam of boron clusters on graphite, pull off the graphene layers in a standard fashion [2], and start to analyze the resulting patterns. Depending on the intensity of that cluster source, there might be copies of roughly the same pattern in neighboring graphene layers. The first results might be nothing more than similar copies of large speckle patterns, but the technique could certainly be refined, step by step.

With such a procedure in mind, we decided to make our model system slightly more realistic by assuming that the layout of small boron clusters might not be too precise. Therefore the resulting boron chains could easily be interrupted

[7] Optimized k-point meshes for graphene ($10 \times 10 \times 3$), zigzag ribbon 1 ($6 \times 3 \times 3$) and 2 ($3 \times 3 \times 3$), armchair ribbon 1 ($2 \times 5 \times 2$) and 2 ($2 \times 3 \times 3$), doped armchair ribbon ($2 \times 3 \times 3$) and doped graphene ($2 \times 3 \times 3$), using the notation of table 1.

by carbon honeycombs, thus forming alternating boron chains running across a suitable bulky graphene nanostructure. This leads us to the model system shown in figure 2(a), where a B_7-cluster has been implanted in the interior of the armchair nanoribbon of figure 1, and the implanted boron clusters within neighboring unit cells are separated by a carbon honeycomb. Note that if we reduce the huge horizontal distance in the x-direction between neighboring nanoribbons, such that the left border of the nanoribbon shown in figure 2(a) would come into bonding distance with its right border (periodic boundary conditions), we obtain a structure model for boron doped bulk graphene, where parallel lines of alternating cluster chains run in the vertical y-direction of figure 2(a), but their mutual distances in the horizontal x-direction are rather large.

We would like to emphasize that the configuration shown in figure 2(a) is not the starting configuration, but already the final relaxed configuration for a boron doped nanoribbon. The final structure of boron doped graphene is almost identical to this picture, and therefore we decided not to depict this structure in figure 2. The fact that the starting configurations and the optimized configurations are so similar may certainly be taken as a strong indication that the basic chemistry of both components must be compatible. Furthermore, the cohesive energies shown in table 1 for these system are in a range that one would expect from a stable implantation of a small boron cluster into bulk graphene nanomaterials.

The most interesting properties of these compound systems are, of course, their basic electronic properties. In figures 2(b) and (d) we see that for the boron doped armchair nanoribbon and for boron doped graphene, the corresponding density of states predicts a metallic behavior, whereas in figure 1(d) for the non-doped armchair nanoribbon, we would find an electronic gap at the same place. The reason for the absence of a gap in the case of the boron doped systems is the two overlapping bands shown in figures 2(c) and (e). The remaining features of the band structure and density of states remain similar to the ones for non-doped armchair graphene shown in figures 1(d) and (f). This may be taken as an indication that the appearance of Bloch states at the Fermi level with crystal momentum $\vec{k}$ in a direction parallel to the alternating boron chains is a rather robust and dominant effect.

Note that in the case of the doped armchair nanoribbons, the bands for Bloch states with $\vec{k}$-vectors in the horizontal x-direction (spanning the width of the nanoribbons) are flat, due to a large lattice parameter chosen to isolate them from neighboring nanoribbons. But in the case of boron doped graphene, where those nanoribbons have been shortcircuited, we have a conduction band pulled down below the Fermi level for Bloch states with $\vec{k}$-vectors in the horizontal x-direction (at right angles to the direction of the alternating boron chains), which might be coupled to Bloch states with $\vec{k}$-vectors in the vertical y-direction parallel to the alternating boron chains. But these features could as well be a reminder of the metallic behavior of the underlying graphene matrix.

At this point, a naive picture emerges of a nanotechnology with conducting 'dotted' lines of boron clusters running through a broad piece of graphene, thus connecting parts of these sheets that act as a basic semiconducting substrate for nanoelectronic devices. Nevertheless, for various reasons this picture might be misleading, and therefore a simple study like the present one certainly needs to be supplemented by further and more detailed research in the near future.

First of all, with our methods we could not determine the nature of the states around the Fermi levels shown in figure 2. They could be extended states, or localized states provided by the embedded boron clusters. The former would lead to metallic conductivity, the latter to hopping conductivity. We could even have a mixed situation of hopping and metallic conductivity along the alternating cluster chains.

Second, it has recently been shown that spin polarization effects absent from our LDA calculations may lead to a band splitting for metallic (zigzag) nanoribbons, thus opening a gap around the Fermi level [24]. We therefore repeated some of our calculations using spin polarized DFT. It turned out that in the case of (boron doped) armchair nanoribbons, there was no qualitative difference to the results shown in figure 2, and that is why we restricted our discussions to the results obtained with the non-polarized LDA.

Finally there are other fundamental aspects that could not be treated in the framework of such a simple study, such as the determination of the distance between boron clusters in the periodic direction, where the metallic behavior might finally disappear. Other interesting topics could be the implantation of even larger boron clusters, or the modeling of inhomogeneous or disordered cluster chains. With small modifications of the present model, and given sufficient computational resources, all of these questions might be answered soon.

Acknowledgments

We would like to thank the staff at the HLR Stuttgart for their assistance during our extensive use of the HLRS supercomputing facilities, and we are particularly indebted to Dr F Gähler from ITAP Stuttgart for introducing us to the handling of the local VASP installations at the HLRS. CÖ also acknowledges financial support by HPC Europe, and JK acknowledges support from the International Max Planck Research School for Advanced Materials (IMPRS-AM).

References

[1] Dresselhaus M S, Dresselhaus G and Eklund P 1996 *Science of Fullerenes and Carbon Nanotubes* (San Diego, CA: Academic)
[2] Novoselov K, Geim A K, Mozorov S V, Jiang D, Zhang Y, Dubonos S V, Grigorieva I V and Firsov A A 2004 *Science* **306** 666
[3] Saito R, Dresselhaus G and Dresselhaus M S 1998 *Physical Properties of Carbon Nanotubes* (London: Imperial College Press)
[4] Nakada K, Fujita M, Dresselhaus G and Dresselhaus M S 1996 *Phys. Rev.* B **54** 17954
[5] Quandt A and Boustani I 2005 *ChemPhysChem* **6** 2001
[6] Kunstmann J and Quandt A 2004 *J. Chem. Phys.* **121** 10680
[7] Pauling L 1960 *The Nature of the Chemical Bond* (Ithaca, NY: Cornell University Press)
[8] Exner K and von Ragué Schleyer P 2000 *Science* **290** 1937
[9] Boustani I 1997 *Phys. Rev.* B **55** 16426
[10] Kunstmann J and Quandt A 2006 *Phys. Rev.* B **47** 035413
[11] Kresse G and Furthmüller J 1996 *Comput. Mater. Sci.* **6** 15

[12] Kresse G and Furthmüller J 1996 *Phys. Rev.* B **54** 11169
[13] Kohn W and Sham L 1965 *Phys. Rev.* B **140** 1133
[14] Teter M P, Payne M C and Allan D C 1989 *Phys. Rev.* B **40** 12255
[15] Perdew J P and Zunger A 1981 *Phys. Rev.* B **23** 5048
[16] Ceperley D and Alder B 1980 *Phys. Rev. Lett.* **45** 566
[17] Vanderbilt D 1990 *Phys. Rev.* B **41** 7892
[18] Kresse G and Hafner J 1994 *J. Phys.: Condens. Matter* **6** 8245
[19] Methfessel M and Paxton A T 1989 *Phys. Rev.* B **40** 3616
[20] Blöchl P E, Jepsen O and Andersen O K 1994 *Phys. Rev.* B **49** 16223
[21] Martins T B, Miwa R H, da Silva A J R and Fazzio A 2007 *Phys. Rev. Lett.* **98** 196803
[22] Hernandez E, Ordejon P, Boustani I, Rubio A and Alonso J A 2000 *J. Chem. Phys.* **113** 3814
[23] Kirkby K, Gwillan R, Smith A and Chivers D 2006 *Ion Implantation Technology: Proc. 16th Int. Conf. on Ion Implantation Technology* (New York: AIP Press)
[24] Son Y W, Cohen M L and Louie S G 2007 *Nature* **444** 347